11th International Symposium on Magnetic Bearings
August 26-29, Nara, Japan

INVERTER VOLTAGE AND SUSPENSION CHARACTERISTICS OF A BEARINGLESS MOTOR

Miya Amada, Naoya Miyamoto, Takehiro Enomoto, Norimasa Tanabe, Junichi Asama, Akira Chiba, Tadashi Fukao
Dept. of Electrical Engineering, Faculty of Science and Technology, Tokyo University of Science
Noda, Chiba 278-8501 Japan
chiba@rs.noda.tus.ac.jp
Satoru Iwasaki
Dept. of Electrical Engineering, Faculty of Technology, Musashi Institute of Technology
Setagaya, Tokyo, Japan
Masatsugu Takemoto
Dept. of Systems Science and Informatics, Hokkaido University
Sapporo, Hokkaido, Japan

ABSTRACT
A wide magnetic gap consequent-pole type bearingless motor has been developed. The wide magnetic gap makes it difficult to start up and suspend a shaft with reasonable suspension voltage and current. To provide high current, high voltage rating is demanded, although, high voltage causes bad influence on magnetic suspension. In this paper, the authors investigate the start-up and rotational characteristics of a prototype bearingless machine driven by voltage source inverters having the rated voltage of 200V and 100V. When the rated voltage is not suitable, significant problems are occurred. The effectiveness of proper selection in the rated voltage is discussed.

INTRODUCTION
A bearingless motor has been developed as a compact device with functions of rotation and suspension. The bearingless motor can generate torque and magnetic suspension force in one motor, because motor windings and suspension windings are installed in the same stator slots [1]-[15]. Thus, motor magnetic field is used as a bias, then, it realizes downsizing and cost reduction. Generally, PM motors are recognized for high efficiency and high power factor. Consequent-pole type bearingless motors are also one of PM motors, with advantages of high force/current ratio and rotational sensorless operation.

The authors have been developing a bearingless motor with wide magnetic gap of 5mm with respect to its rotor radius of 32mm. To generate the magnetic suspension force with the wide magnetic gaps, considerable current is needed. Thus, high voltage and current ratings are required in a suspension current drive inverter.

In this paper, two types of voltage source PWM inverters are tested. One is 100V, 3A three-phase inverter with a diode rectifier for single phase commercial line. Another is 200V, 11A three-phase inverter with three-phase 200V diode rectifier. The magnetic suspension characteristics and the start-up process are compared experimentally.

At initial stage, it was expected that the 200V inverter would provide better performance. However, it is found that the 100V inverter provides some advantages.

PRINCIPLE OF SUSPENSION FORCE GENERATION
Figure 1 shows a rotor and a stator of a consequent-pole type bearingless motor at the angular position θ_z=0deg. In the rotor, radially magnetized PMs are inset between the rotor iron poles. The PM originated bias fluxes go through the magnetic gaps, a stator and a rotor iron pole. Consequently, the rotor iron poles are magnetized. In this figure, the PM outside is N-pole, so the iron poles between PMs become S-pole. This rotor can work as an 8-pole rotor.

In the figure, the suspension force is generated in the

negative *x*-direction. The Ψ_m is PM bias flux, and the Ψ_x is the magnetic flux caused by the current in suspension winding N_x. The Ψ_x goes through the stator yoke, the air gap and the rotor iron. Thus, the PM bias fluxes and suspension flux are superimposed in the air gap. The suspension force is generated because the flux densities are unbalanced. When a rotor is rotated, the force generation method of the suspension force is the same. The Ψ_x goes through the rotor iron between PMs. The N_x suspension current generates the *x*-axis suspension force at any rotor rotational position. If negative current is provided in the N_x, then, positive *x*-axis suspension force is generated. If the force is needed in the *y*-direction, the current is provided in suspension winding N_y. In the similar manner, the N_y winding current generates *y*-axis suspension force. The total suspension force is generated by a vector sum of the *x*- and *y*-axis forces.

Consequent-pole type bearingless motor can generate constant suspension force despite of the rotor rotational position, because the flux goes through the iron part between the PMs. Thus, the suspension control system is simple. The suspension controller and the motor controller can be independent. The current is small because suspension flux does not go through the PMs having high reluctance.

SYSTEM CONFIGURATION

Figure 2 shows the outline of a prototype machine aimed for the application of a centrifugal pump. This machine has two pairs of rotor and stator, assigned as unit1 and unit2. These are consequent-pole type bearingless motors. The magnetic gaps between rotors and stators are 5mm. The prototype machine has partitions shown in gray colored area to protect from the transportation liquid. Thus, the mechanical gap is 1mm. In Figure 2, the mechanical gap is shown in white colored area.

When the magnetic gaps are wide, it is difficult for the rotor iron poles to be magnetized. In unit1 and unit2, the magnetized PM directions are different. The S-pole PMs are outside in unit1, and the N-pole PMs are outside in unit2. Moreover, there are PMs between bearingless motors which are magnetized shaft direction. The structure enhances suspension force.

There is a disk at the end of unit2 for an axial

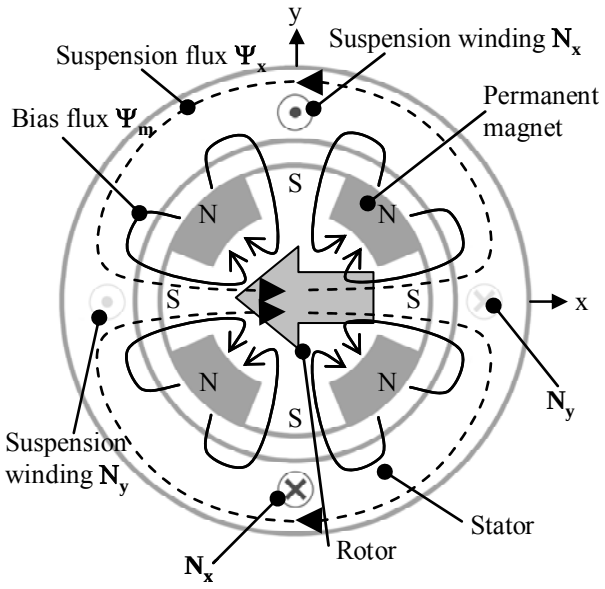

FIGURE 1: Principle of suspension force generation.

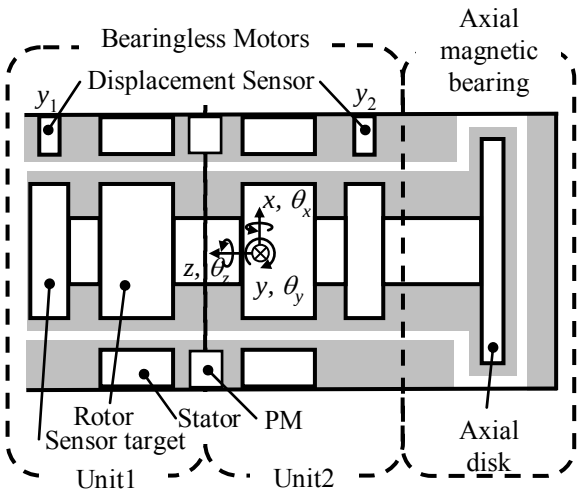

FIGURE 2: Outline of the prototype machine.

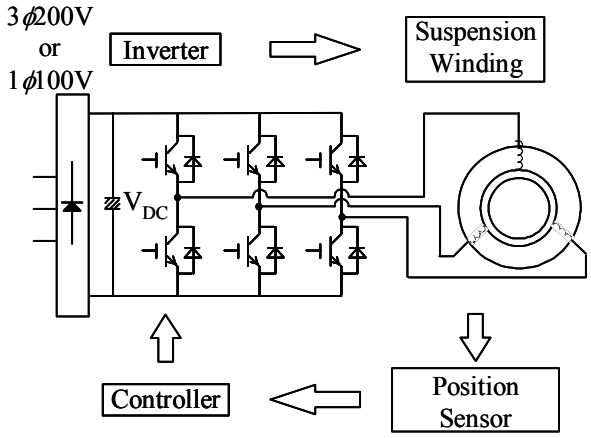

FIGURE 3: Structure of the magnetic suspension controller system.

magnetic bearing. The machine is controlled actively for 5axes. A center of gravity is not at the center of the shaft due to the axial disk. The bearingless motor actively regulates the motion of a center of gravity, both radial (x, y), conical (θ_x, θ_y) and axial (z) motions with five eddy current sensors. The function of the axial disk is only z-axis magnetic suspension. In the rest of this paper, 4-axis positioning is mainly discussed.

In order to regulate the suspension force, a controller and inverters are needed. To drive the PM motor, a general-purpose inverter is employed.

Figure 3 shows a composition of the magnetic suspension controller system. The controller detects the shaft displacements from the position sensors. Then, the controller calculates gate signals of inverter power devices. The currents from the inverter are provided in the suspension windings, and the suspension force is generated. The force can move the rotor, and the movement is detected by the position sensors. Five position sensors are used in this machine. These are x_1 and y_1 for unit1, x_2 and y_2 for unit2 and z for axial movement. The y_1 and y_2 sensors are shown in Figure 2, previously.

Figure 4 shows a block diagram of the controller. These blocks are realized in a microprocessor. The control system has a digital PID controller. In order to compensate for the current delay caused by a coil inductance, the current feedback is constructed. With exact current regulation, the suspension force is controlled to realize magnetic suspension.

The signals from the position sensors are processed by a digital low pass filter to remove the noises. In a controller, the signals from the position sensors are used to calculate the displacements and movements at the center of gravity.

200V INVERTER

In this country, commercial power supply for single phase is 100V. For three-phase power supply, 200V line-to-line is usually used for fractional horse power motors.

In this prototype machine, the magnetic gaps are wide. Therefore, 200V three-phase inverters with DC bus voltage V_{DC} of 280V are initially used for the magnetic suspension. The current rating is 11A. However, there are some problems using this high voltage inverter.

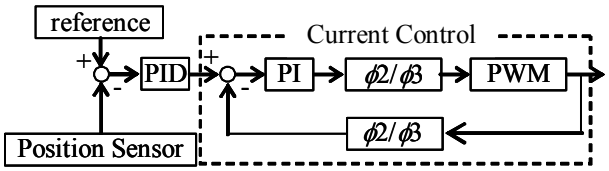

FIGURE 4: Controller block diagram.

TABLE 1: Comparison of inverters.

	width	depth	height
200V INV.	650	240	190
100V INV.	420	100	157

(a) The physical size and dimensions of the inverter is considerable.
(b) The inverter is expensive.
(c) The switching noises are apparent.

EXPERIMENTAL METHOD

Two types of inverters are used in the experiments. One is the 200V 11A inverter with V_{DC} of 280V and another is the 100V 3A inverter with V_{DC} of 140V. The current ratings are in continuous operations. Both inverters can provide a few times of current for a short period. The dimensions of these inverters are compared in Table 1. The dimensions of inverters include sensor interface, controllers, two units of three-phase inverters and a general-purpose motor drive inverter. The volume of the 200V inverters is more than 4 times of that of the 100V inverters.

The suspension inverter adjustment is mostly the same in experiments, except the current control gains and the dead time. The dead time and the current control gains are optimized for each inverter. The current control gains are optimized for corresponding inverter voltages.

START-UP CHARACTERISTICS

Figure 5 shows the radial x- and y-axis displacements at start-up from 1mm. In this figure, x_1, y_1, x_2 and y_2 are signals of the position sensors of unit1 and unit2, respectively. The PID gains for the suspension control are kept at the same value. The references of displacement and angle are 0mm and 0rad. These experiments are done at the same rotational position, i.e.,

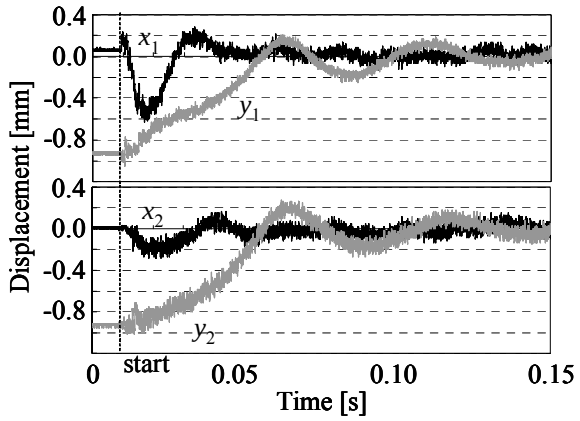

(a) Waveforms with 200V inverter.

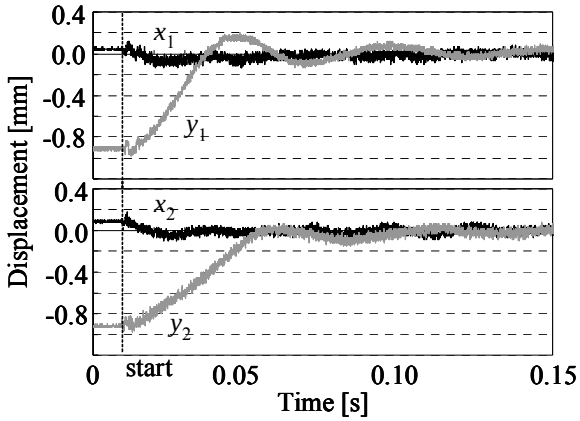

(b) Waveforms with 100V inverter.

FIGURE 5: Radial positions at start-up.

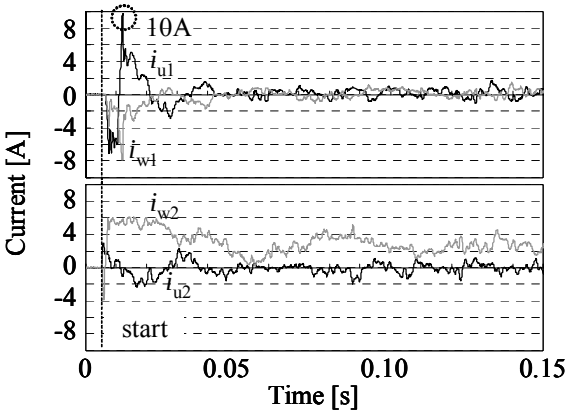

(a) Waveforms with 200V inverter.

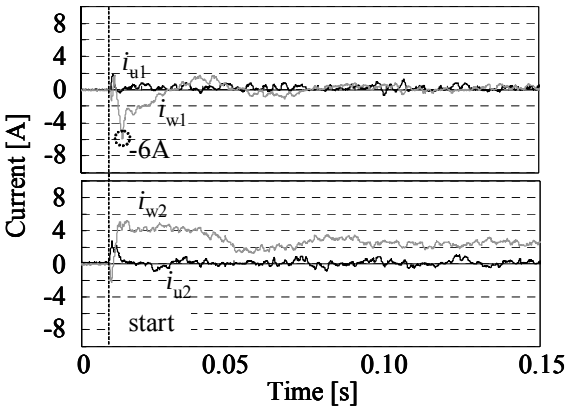

(b) Waveforms with 100V inverter.

FIGURE 6: Suspension winding currents at start-up.

θ_z is 0deg. Before starting, the rotor is displaced about -1mm in *y*-axis because of the gravity and the magnetic unbalanced force. When the suspension driver is switched on, the rotor moves to center positions.

In radial position waveforms before and after the start-up, the thicknesses of waveforms are increased because of the noises. It is seen that the noises are reduced with the 100V inverter.

Figure 6 shows the waveforms of the suspension winding currents at the start-up. In these figures, i_{u1} i_{w1}, i_{u2} and i_{w2} are suspension winding currents of u- and w-phase in the unit1 and unit2, respectively. These currents are measured by current probes. In unit1 and unit2, the current directions are different. The positive x-axis suspension force is generated by the positive i_{u2} current and the negative i_{u1} current. These figures show that the shaft can start up successfully with both inverters.

Figure 7 shows the waveforms of the displacements and the currents at the start-up. The upper displacement shows the shaft movements of the center of gravity. The controller regulates the positions of the center of gravity. The *y* is derived from the sensor outputs of y_1 and y_2 by the following equation;

$$y = \frac{L_{s2} y_1 + L_{s1} y_2}{L_{s1} + L_{s2}} \quad \text{.....(1)}$$

The L_{s1} and L_{s2} are the distances of each sensor from the shaft center of gravity. The response time of the 200V inverter and the 100V inverter are 0.095s and 0.080s, respectively.

In Figure 7, the i_{b2} waveforms of the suspension currents are also shown. These currents are in 2-phase coordinate. These are calculated from the suspension winding currents by the following equation;

$$i_{v2} = -i_{u2} - i_{w2} \quad \text{..... (2)}$$

$$\begin{bmatrix} i_{a2} \\ i_{b2} \end{bmatrix} = \sqrt{\frac{2}{3}} \begin{bmatrix} 1 & -\frac{1}{2} & -\frac{1}{2} \\ 0 & \frac{\sqrt{3}}{2} & -\frac{\sqrt{3}}{2} \end{bmatrix} \begin{bmatrix} i_{u2} \\ i_{v2} \\ i_{w2} \end{bmatrix} \quad \text{..... (3)}$$

The suspension force that supports the shaft weight and the PM force is necessary for *y*-axis. The i_{b2} is mainly responsible to generate the start-up magnetic force. In the steady state, the current value of 4A is necessary to suspend the shaft weight. In this experiment, the reference of displacement is 0mm. When the reference is properly adjusted, the current can be less because the magnetic unbalanced force helps to suspend the shaft.

The maximum currents of the 200V inverter and the 100V inverter are set about 10A and 6A, respectively. In the 100V inverter, the current is limited by the power devices in the inverter. The start-up with the 100V inverter is slightly faster than that with the 200V inverter. In the 200V inverter, a large current of 10A is provided instantaneously. At the same magnetic suspension loop gain, the waveforms of displacement are not the same. This is related to the current and voltage limits.

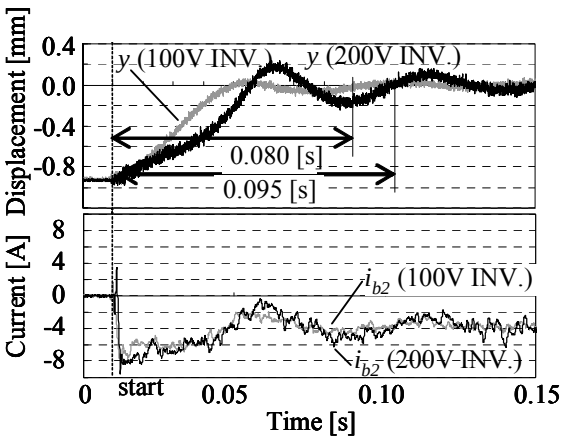

FIGURE 7: Comparison of the start-up response in two inverters.

ROTATION CHARACTERISTICS

By using a commercially available three-phase pulse-width-modulation (PWM) inverter, the consequent-pole bearingless PM motor is driven up to 6,000min^{-1}. Figure 8 (a) shows vibration amplitudes of the magnetically levitated rotor. The vibration amplitudes of *x*, *y*, θ_x and θ_y with the 200V inverter and the 100V inverter are compared. The measurements are carried out every 300min^{-1} until 6,000min^{-1}. In both inverters, remarkable resonance or unstable behavior is not observed expect 300min^{-1}.

Figures 8 (b) and (c) show displacement waveforms of the *y*-axis at 300min^{-1} with the 200V inverter and the 100V inverter, respectively. The amplitude is shown in the broken line in this figure. The position reference is set to 0.1mm. The 3σ displacement variations with the 200V inverter are about 0.14mm at 300min^{-1}, which is one seventh the touchdown clearance of 1mm. It is seen that the vibration amplitudes are relatively small compared to movable limitations in the radial and tilting directions of 1mm and 6mrad, respectively. The amplitudes with the 200V inverter are larger than those with the 100V inverter.

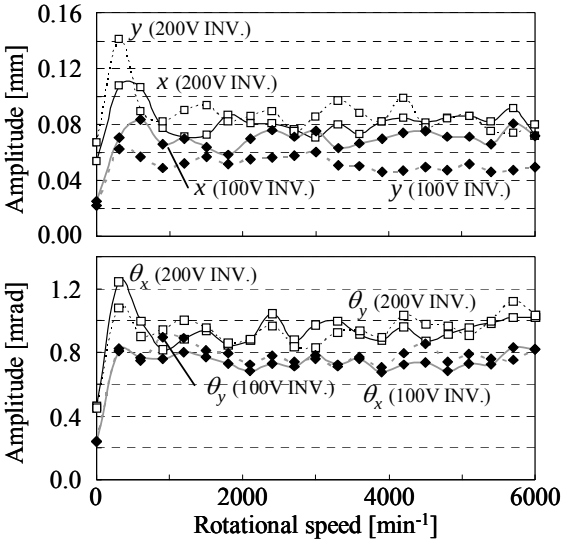

(a) Vibration amplitudes.

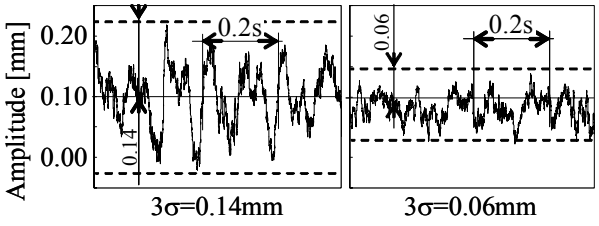

(b) Displacement waveform with 200V inverter.

(c) Displacement waveform with 100V inverter.

FIGURE 8: Rotation vibration amplitudes.

In this machine, the suspension feedback bandwidth is designed the same as each other. However, the vibration amplitude is different.

COMPARISON OF TWO INVERTERS

In the prior sections, the start-up characteristics and rotational vibration characteristics are compared when suspension windings are driven by the 100V or the 200V inverters. At the initial stage, the authors expected better performance with the 200V inverter. In the rotational test, shaft fluctuation is large with the 200V inverter. In the start-up process, not much difference is seen.

In this section, the difference of two types of inverters is discussed. One of the differences in using these inverters is the noises. Figure 9 shows the waveforms of the *x*-axis position at standstill. In the waveform with the 200V inverter, the noises are composed of low frequencies 10Hz-30Hz, middle frequencies 2kHz-20kHz and high frequencies 100kHz. The middle frequency noises are originated from PWM carrier frequency. As the voltage is high, the slew rate is high, resulting electrical and magnetic interference. With the 100V inverter, the noise level is rather low.

The other difference of two inverters is the current response. Figure 10 (a) shows the step current responses of each inverter. The settling time is 1.2ms when the amplitude of step current is 0.8A. This current value is rather small, thus current responses are the mostly the same. The current controller gains are adjusted so that small step responses are close to each other.

When a large step current is required, there is a significant difference in the 200V and the 100V inverters. Figure 10 (b) shows the step current responses when the amplitude of step current is 6A. The settling time is 2.75ms. Fast current slew rate is obvious in 200V inverter as expected. However, significant overshoot is also observed. Despite of current gain adjustment, better response can not be observed. The current responses may be related to CPU calculation speed. The CPU has 100μs and 200μs interrupts. The differences of this slope and the overshoot are significant difference of two inverters.

In addition, these inverters have different resolution in current sensors. The 200V inverter can handle 31.25A current, with 12bit A/D converter. On the contrary, the 100V inverter is for 8A at 12 bit resolution.

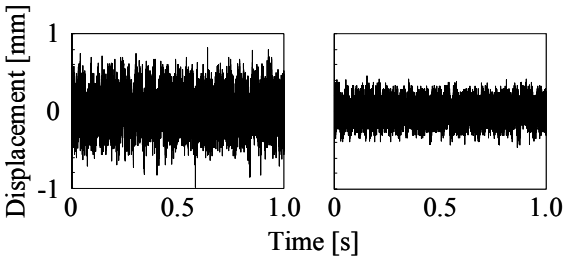

FIGURE 9: The noises in steady state.

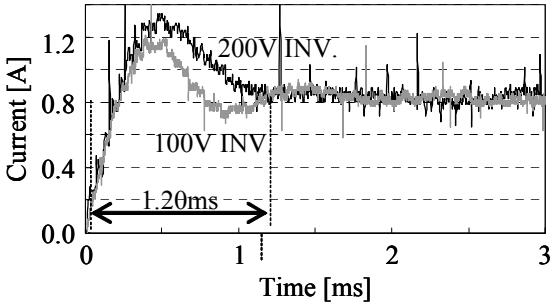

(a) Step current response of 0.8A.

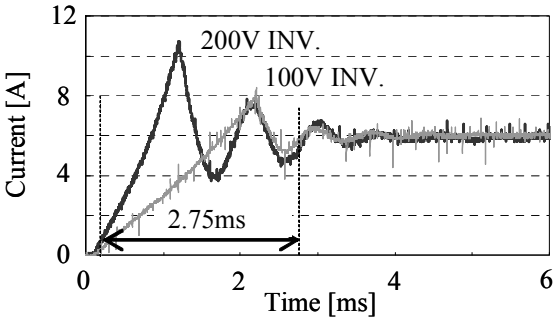

(b) Step current response of 6A.

FIGURE 10: The step current responses

CONCLUSION

In this paper, two types of voltage source inverters are adapted in magnetic suspension current drive. The inverters have a diode rectifier. One is for single phase 100V and another is three-phase 200V. At the design stage the performance with the 200V inverter is expected to be better although the cost is high and dimensions are large. However, in experiments, the 100V inverter provided better performance in a few aspects. It is found that the noise is low with 100V inverter. In the rotational test, shaft displacements are

less with the 100V inverter.

The 100V inverter is suitable for this prototype machine. The reasons are summarized as,

(a) The physical size and dimensions of the inverter is small.
(b) The inverter is less expensive.
(c) The noise level is less.
(d) The shaft vibration is small in rotation.

References

1. Oguri, K., Watada, M., Torii, S. and Ebihara, D., Design Optimization of Magnetic Bearing Composed of Permanent Magnets for the Bearing-Less Motor, Proc. of the 7th Int. Symp. on Magnetic Bearings, ETH Zurich, Switzerland, Aug. 2000.
2. Kanebako, H. and Okada, Y., New Design Of Hybrid Type Self-Bearing Motor for High-speed Miniature Spindle, Proc. of the 8th Int. Symp. on Magnetic Bearings, Mito, Japan, 2002.
3. Gomrd, R. R., Stephan, R. M. and Santisteban, J. A., Self-bearing Motor with DSP Based Control System, Proc. of the 10th Int. Symp. on Magnetic Bearing, Martigny, Switzerland, Aug. 2006.
4. Neff, M., Barletta, N. and Schob, R., Bearingless Centrifugal Pump for Highly Pure Chemicals, Proc. of the 8th Int. Symp. on Magnetic Bearings, Mito, Japan, 2002.
5. Steele, B. and Stephens, L., A Test Rig for Measuring Force and Torque Production in a Lorenz Slotless Self Bearing Motor, Proc. of the 7th Int. Symp. on Magnetic Bearings, ETH Zurich, Switzerland, Aug. 2000.
6. Stephens, L. S. and Dae-GOn Kim, Force and torque characteristics for a slotless Lorentz self-bearing servomotor, IEEE Trans. Magnetics vol.38, pp.1764-1773, Jul. 2002.
7. Khoo, W. K. S., Bridge Configured Winding for Polyphase Self-Bearing Machines IEEE Trans. Magnetics vol.41, pp.1289-1295, Apr. 2005.
8. Zhang T., Zhu, H. and Sun, Y., Rotor Suspension Principle and Decoupling Control for Self-bearing Induction Motors, Conf. Power Electronics and Motion Control vol.1 pp1-5, Aug. 2006.
9. Horz, M., Herzog, H.-G. and Mendler, N., System design and comparison of calculated and measured performance of a bearing less BLDC-drive with axial flux path for an implantable blood pump, Conf. Power Electronics, Electrical Drives Automation and Motion, pp.1025-1027, May 2006.
10. Grabner, H., Amrhein, W., Silber, S. and Nenninger, K., Nonlinear Feedback Control of a Bearingless Brushless DC Motor, Conf. Power Electronics and Derives Systems, vol.1 pp366-371 Jan. 2006.
11. Schneider, T. and Binder, A., Design and Evaluation of a 60,000 rpm Permanent Magnet Bearingless High Speed Motor, Conf. Power Electronics and Derives Systems pp.1-8 Nov. 2007.
12. Chiba, A., Fukao, T., Ichikawa, O., Oshima, M., Takemoto, M. and Dorrell, D. G., Magnetic Bearings and Bearingless Drives, Newnes Elsevier 2005, Mar. 381pages ISBN 0 7506 5727 8
13. Oshima, M., Miyazawa, S., Deido, T., Chiba, A., Nakamura, F. and Fukao, T., Characteristics of a Permanent Magnet Type Bearingless Motor IEEE Trans. Industry applications, vol.32, No.2, pp.363-370, Apr. 1996.
14. Amemiya, J., Chiba, A., Dorrell. D. G. and Fukao, T., Basic Characteristics of a Consequent-Pole-Type Bearingless Motor, IEEE Trans. Magnetics, vol.41 No.1 pp.82-89, Jan. 2005.
15. Asami, K., Chiba, A., Rahman, M. A., Hoshino, T. and Nakajima, A., Stiffness Analysis of Magnetically Suspended Bearingless Motor With Permanent Magnet Passive Positioning IEEE Trans. Industry Applications vol.41, No.10, pp.3820-3822, Oct. 2005.